Irrigated Agriculture Significantly Modifies Seasonal Boundary Layer Atmosphere and Lower-Tropospheric Convective Environment

EMILEE LACHENMEIER,[a,b] REZAUL MAHMOOD,[a,b] CHRIS PHILLIPS,[c] UDAYSANKAR NAIR,[c] ERIC RAPPIN,[d] ROGER A. PIELKE SR.,[e,f] WILLIAM BROWN,[g] STEVE ONCLEY,[g] JOSHUA WURMAN,[h] KAREN KOSIBA,[h] AARON KAULFUS,[c] JOSEPH SANTANELLO JR.,[i] EDWARD KIM,[i] PATRICIA LAWSTON-PARKER,[i,j] MICHAEL HAYES,[b] AND TRENTON E. FRANZ[b]

[a] *High Plains Regional Climate Center, University of Nebraska–Lincoln, Lincoln, Nebraska*
[b] *School of Natural Resources, University of Nebraska–Lincoln, Lincoln, Nebraska*
[c] *Department of Atmospheric Science, University of Alabama in Huntsville, Huntsville, Alabama*
[d] *Kentucky Climate Center, Western Kentucky University, Bowling Green, Kentucky*
[e] *Department of Atmospheric and Oceanic Sciences, University of Colorado Boulder, Boulder, Colorado*
[f] *Cooperative Institute for Research in Environmental Sciences, University of Colorado Boulder, Boulder, Colorado*
[g] *Earth Observation Laboratory, National Center for Atmospheric Research, Boulder, Colorado*
[h] *University of Illinois Urbana–Champaign, Urbana, Illinois*
[i] *NASA Goddard Space Flight Center, Greenbelt, Maryland*
[j] *Earth System Science Interdisciplinary Center, University of Maryland, College Park, College Park, Maryland*

(Manuscript received 5 February 2023, in final form 19 November 2023, accepted 4 December 2023)

ABSTRACT: Modification of grasslands into irrigated and nonirrigated agriculture in the Great Plains resulted in significant impacts on weather and climate. However, there has been lack of observational data–based studies solely focused on impacts of irrigation on the PBL and convective conditions. The Great Plains Irrigation Experiment (GRAINEX), conducted during the 2018 growing season, collected data over irrigated and nonirrigated land uses over Nebraska to understand these impacts. Specifically, the objective was to determine whether the impacts of irrigation are sustained throughout the growing season. The data analyzed include latent and sensible heat flux, air temperature, dewpoint temperature, equivalent temperature (moist enthalpy), PBL height, lifting condensation level (LCL), level of free convection (LFC), and PBL mixing ratio. Results show increased partitioning of energy into latent heat relative to sensible heat over irrigated areas while average maximum air temperature was decreased and dewpoint temperature was increased from the early to peak growing season. Radiosonde data suggest reduced planetary boundary layer (PBL) heights at all launch sites from the early to peak growing season. However, reduction of PBL height was much greater over irrigated areas than over nonirrigated croplands. Relative to the early growing period, LCL and LFC heights were also lower during the peak growing period over irrigated areas. Results note, for the first time, that the impacts of irrigation on PBL evolution and convective environment can be sustained throughout the growing season and regardless of background atmospheric conditions. These are important findings and applicable to other irrigated areas in the world.

SIGNIFICANCE STATEMENT: To meet the ever-increasing demand for food, many regions of the world have adopted widespread irrigation. The High Plains Aquifer (HPA) region, located within the Great Plains of the United States, is one of the most extensively irrigated regions. In this study, for the first time, we have conducted a detailed irrigation-focused land surface and atmospheric data collection campaign to determine irrigation impacts on the atmosphere. This research demonstrates that irrigation significantly alters lower atmospheric characteristics and creates favorable cloud and convection development conditions during the growing season. The results clearly show first-order impacts of irrigation on regional weather and climate and hence warrant further attention so that we can minimize negative impacts and achieve sustainable irrigation.

KEYWORDS: Atmosphere–land interaction; Biosphere–atmosphere interaction; Land use; Convection; Boundary layer; Mesoscale processes

1. Introduction

A number of studies in the past investigated impacts of land-use/land-cover change (LULCC) on weather and climate around the world (Gullison et al. 2007; Pielke et al. 2007, 2011, 2016; Mahmood et al. 2014; Melillo et al. 2014; IPCC 2019; McDermid et al. 2023). Climate variables impacted include temperature, moisture content, surface short- and longwave radiation, and atmospheric turbulence, which impacts momentum, heat, water vapor, and carbon dioxide fluxes (Bala et al. 2007; Paul et al. 2016; Nair et al. 2019; Yamada and Pokhrel 2019; He et al. 2020; Kuttippurath et al. 2021; Maeda et al. 2021). A subset of these research addressed the role of LULCC on the weather and climate of the Great Plains (GP) (Mahmood and Hubbard 2002; Adegoke et al. 2003;

Supplemental information related to this paper is available at the Journals Online website: https://doi.org/10.1175/JAMC-D-23-0020.s1.

Corresponding author: Rezaul Mahmood, rmahmood2@unl.edu

DOI: 10.1175/JAMC-D-23-0020.1

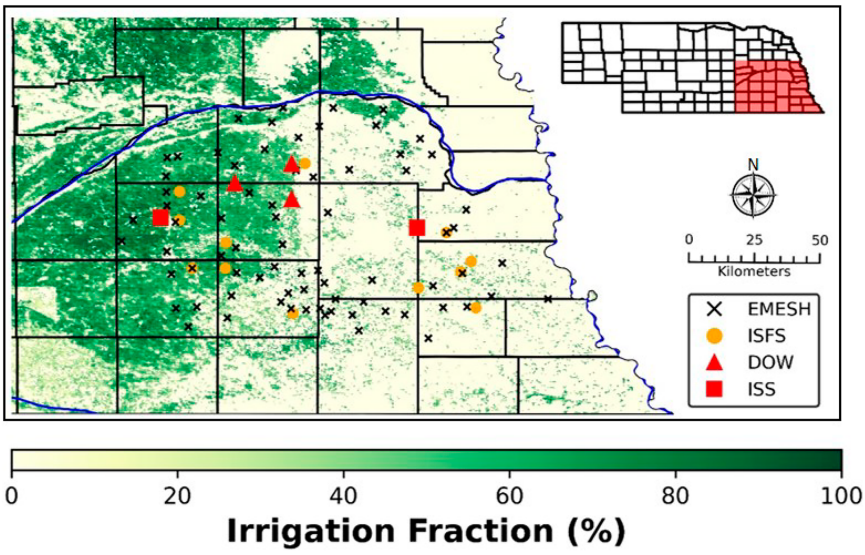

FIG. 1. Map of the GRAINEX study area in southeastern Nebraska. Data collection sites consisted of the 12 integrated surface flux system sites (ISFS), 2 integrated sounding system sites (ISS), 3 Doppler on Wheels deployment locations (DOW), and the 75 Environmental Monitoring, Economical Sensor Hubs (EMESH).

DeAngelis et al. 2010; Qian et al. 2013, 2020; Lawston et al. 2015; Mueller et al. 2016; Alter et al. 2018; Zhang et al. 2019; Szilagyi and Franz 2020; Yang et al. 2020, 2019). Observations show that a large swath of land used for agriculture in the High Plains Aquifer (HPA) region of the central United States (South Dakota, Nebraska, Kansas, Oklahoma, Texas, Wyoming, Colorado, and New Mexico) is irrigated (Brown and Pervez 2014; Ajaz et al. 2020). Increased application of water associated with irrigation modifies energy partitioning by reducing sensible heat flux, increasing latent heat flux and suppressing maximum air temperature values (Kang and Bryan 2011; Seneviratne et al. 2006; Huber et al. 2014; Diffenbaugh 2009). As a result, for example, a general cooling in daytime air temperatures has been observed over irrigated regions (Gameda et al. 2007; Mueller et al. 2017; Alter et al. 2018; Mahmood et al. 2004, 2006, 2013). Based on these observations it can also be inferred that irrigation driven LULCC in the GP (and elsewhere in the world) potentially alter planetary boundary layer evolution and convective environment.

To further explore these unknowns and understand the impacts of the LULCC due to irrigation, the Great Plains Irrigation Experiment (GRAINEX) was conducted in Nebraska in 2018 (Fig. 1). Results from this study have global implications because irrigated agriculture has expanded rapidly around the world since the mid-twentieth century with the so-called green revolution and potentially will continue to further expand over the coming decades to meet the global demand for food. In addition, to the best of our knowledge, this is the first field campaign solely focused on impacts of irrigation on land–atmosphere (L-A) interactions. This study, for the first time and based on observational data, identified the impacts of irrigation on convective environment throughout the growing season (late May through early August), as opposed to under specific days with certain background atmospheric conditions, and when land surface condition also changed in response to crop growth and its water demand. In addition, the study region represents an area where nonirrigated agricultural land transitions into widespread irrigated agricultural land (Mahmood and Hubbard 2002; Adegoke et al. 2003; Lawston et al. 2015). The transition from one type of land use to another (nonirrigated to irrigated in this case), provided an additional opportunity to assess the impacts of these land uses on the atmosphere under a unique setting.

The specific objective of this paper is to investigate impacts of irrigated and nonirrigated land use on the latent and sensible heat flux, near-surface air temperature and moisture, planetary boundary layer (PBL) evolution, and changes in convective measures such as lifting condensation level (LCL) and level of free convection (LFC) under clear- and nonclear-sky conditions. The current paper has built and significantly expanded upon the findings of Rappin et al. (2021). The latter paper provided an overview of the GRAINEX field campaign, observation platforms and network; and discussed overall land surface conditions over irrigated and nonirrigated land uses and their influences. In addition, Rappin et al. (2021) presented detailed assessment of evolution of the planetary boundary layer during 22–24 July 2018, over irrigated and nonirrigated areas. On the other hand, the current paper presents results from the analysis of data from the entire field campaign including early and midgrowing seasons over irrigated and nonirrigated land use and demonstrate their influence on the near-surface meteorology. These periods are referred to as intense observation period 1 (IOP 1: 30 May–13 June 2018; early growing season) and intense observation period 2 (IOP 2: 16–30 July; peak growing season). The window of dates for IOP 1 was chosen in an effort to observe L-A interactions amid the early onset of irrigation

TABLE 1. GRAINEX ISFS sites and their locations (source: Rappin et al. 2021). All sites are located in Nebraska.

Site	Nearest town	Lat (°N)	Lon (°E)	LULC	Flux sensor mounting height (m)
1	Benedict	41.00	−97.54	Irrigated	6
2	York	40.88	−97.54	Irrigated	6
3	Exeter	40.66	−97.48	Irrigated	6
4	Beaver Crossing	40.78	−97.33	Irrigated	6
5	Friend	40.66	−97.33	Irrigated	6
6	Wilber	40.46	−97.03	Irrigated	6
7	Loma	41.14	−96.97	Nonirrigated	4.5
8	Panama	40.57	−96.46	Nonirrigated	6.5
9	Elmwood	40.82	−96.34	Nonirrigated	6.5
10	Unadilla	40.65	−96.27	Nonirrigated	6.5
11	Unadilla	40.69	−96.22	Nonirrigated	4.5
12	Cook	40.48	−96.20	Nonirrigated	5.5

(i.e., a rapid increase in moisture availability in both surface and subsurface regions). IOP 2 was chosen to capture L-A interactions during the peak growing season when the irrigation amount is maximized in response to crop-water demand. In the paper, IOP 1 and the early growing season and IOP 2 and the peak growing season are used interchangeably.

2. Data and methods

a. *Field campaign and observation platforms*

The GRAINEX field campaign was conducted in southeast Nebraska from late May through early August of 2018. Nebraska, located within the North American Great Plains, is one of the most extensively irrigated regions in the world (Bonfils and Lobell 2007; Lobell et al. 2009). The primary source of water is the High Plains Aquifer, which is also known as the Ogallala Aquifer. As shown in Fig. 1, an extensive area of irrigated cropland is found in the western part of the study area and nonirrigated rainfed cropland is generally found to the east. Corn and soybeans are prevalent crops in the study area. During the field campaign, IOP 1 experienced several rain events (Rappin et al. 2021). This condition also resulted in periods of cooler and drier days. Like IOP 1, IOP 2 also experienced periodic sunny and partly sunny conditions alternated by showers and thunderstorms (Rappin et al. 2021).

A wide range of observational platforms were used for data collection. These included 12 eddy covariance Integrated Surface Flux Systems (ISFS; NCAR Earth Observing Laboratory 1990), 2 Integrated Sounding Systems (ISS; NCAR Earth Observing Laboratory 1997), and 3 Doppler on Wheels (DOW) mobile radar units (Wurman et al. 2021), which also deployed radiosondes and Environmental Monitoring, Ecological Sensor Hubs (EMESH; Rappin et al. 2021). The National Aeronautics and Space Administration (NASA) also participated by collecting soil moisture data using radiometers mounted on a Twin Otter aircraft. This paper focuses on the analyses of data from the ISFS, ISS, and DOW platforms, and hence we will not discuss EMESH and NASA data. Description of the instrumentation, data collected, and quality of data collected by ISFS, ISS, and DOW are discussed in the following sections. [For additional details on all observation platforms and instrumentation, see online (https://www.eol.ucar.edu/field_projects/grainex).]

b. *ISFS*

A total of 12 ISFS sites were deployed for the GRAINEX campaign (Tables 1 and 2). Six sites were deployed in irrigated crop environments, six in nonirrigated (Fig. 1). The six irrigated sites were located in the western irrigated part of the study area (i.e., west of the Big Blue River), and the remaining six were in the eastern nonirrigated part. The meteorological parameters measured at the ISFS sites included latent and

TABLE 2. Parameters measured at each GRAINEX ISFS site (source: Rappin et al. 2021).

Parameter	Sensor	Mounting height/depth (m)
Air temperature; relative humidity	NCAR TRH	2
Air pressure	Vaisala PTB220 and PTB2010 barometers; Paroscientific nanobarometer	2
Fluxes of momentum, sensible and latent heat, and carbon dioxide	Campbell CSAT3A/EC150	4.5–6
Horizontal wind speed/direction	Gill WindObserver 2D sonic anemometer	10
Precipitation (rain)	MRI tipping bucket	2
Radiation (four components)	Hukseflux NR01 integrated radiometer	2
Soil heat capacity	Hukseflux TP01	0.025
Soil heat flux	REBS HFT	0.05
Soil moisture	Decagon EC-5	0.025
Soil temperature profile	NCAR Tsoil	0–0.05

TABLE 3. Measurements at the ISS location: nonirrigated Rogers Memorial Farm (latitude 40.84°N, longitude 96.47°W) and irrigated York Municipal Airport (latitude 40.89°N, longitude 97.63°W).

System	Measurement	Sensor
Upper air	Cloud height	Vaisala CL31 and CL51 ceilometer
	Sounding variables	Vaisala MW41/RS 41 radiosondes
	Wind profile	LAP3000 915 MHz DBS radar wind profiler with RASS
Surface	Pressure	Vaisala PTB210
	Radiation (four components)	Hukseflux NR01
	Precipitation (rain)	HAS tipping bucket
	Meteorological summary: temperature, relative humidity, precipitation type, precipitation intensity, precipitation quantity, air pressure, wind direction, wind speed, and radiation	Lufft WS700/800 weather sensors

sensible heat fluxes, air temperature, relative humidity, pressure, precipitation, wind speed, wind direction, incoming and outgoing solar radiation, and soil moisture. The entire dataset was quality-controlled and released to the NCAR Earth Observing Laboratory data portal as 5-min averages in NetCDF format (https://www.eol.ucar.edu/observing_facilities/isfs).

c. ISS

In addition to the ISFS sites, two ISS sites were assigned in an effort to capture anomalies in the PBL associated with irrigated and nonirrigated agricultural practices (Table 3). One ISS site was located at the York Airport in York, Nebraska, a small airfield in the area. Nearby crop fields are extensively irrigated and radiosonde launches were conducted in an area removed from runway activities. The second ISS site was located at Rogers Memorial Farm (Rogers Farm), a test farm east of Lincoln that is owned and operated by the University of Nebraska. This site lies within the confines of the nonirrigated ISFS sites. Radiosonde launches took place simultaneously at 2-h intervals from sunrise [approximately 0500 local standard time (LST)] to sunset (approximately 1900 LST) each day. Thus, eight radiosonde launches were completed each day from each site resulting in about 480 launches (8 launches × 2 sites × 30 days = 480 launches) over IOPs 1 and 2. These sites also included a wind profiler, a ceilometer and collected surface meteorological observations. At the ISS sites, Vaisala RS41-SGP radiosondes were utilized. Measurement errors (±) for the Vaisala radiosonde are 0.3°C, 4%, 1.0 hPa, 10 m, and 0.15 m s^{-1} for temperature, relative humidity, pressure, height, and wind speed, respectively.

These sites were only operational during IOP 1 and 2, therefore, this analysis of the GRAINEX data highlights events constrained by these time windows. They (ISS 2 and 3) provide the most comprehensive dataset of this type for investigation of impacts of land use, including irrigation, on the lower atmosphere.

d. DOW

Three DOW units were deployed and located over irrigated, nonirrigated and over a transition region between irrigated and nonirrigated land uses (Fig. 1). The DOW sites conducted radiosonde launches, which corresponded to the launch times of the ISS sites (8 launches × 3 sites × 30 days = 720 launches). The DOW sounding sites launched Graw DFM-09 radiosondes bihourly from 0500 until 1900 LST each day of the IOP. These sondes measure temperature, relative humidity, pressure, height, and wind speed. Observation errors (±) are less than 0.2°C, 4% RH, 0.3 hPa, 10 m, and 0.2 m s^{-1}, respectively.

e. PBLH, LCL, and LFC

To compute PBL height (PBLH), the base of the lowest temperature inversion is identified in the sounding data. If this inversion is located at the surface (i.e., the nighttime surface-based inversion), then the top of the inversion is identified as the PBLH. For cases where no inversion is located below 600 hPa, then a parcel mixing method (Seidel et al. 2010) is utilized. In this methodology, a hypothetical surface parcel is displaced vertically until the potential temperature is equivalent to the environment. The height at which this occurs is the PBLH. The 600-hPa threshold for switching from the inversion-based method to the mixing technique is based on visual inspection of the sounding profiles to prevent misidentification of remnant layers as the PBL top. When compared with hand-picked PBLHs for 240 soundings from the ISS 3 site, this methodology produces a correlation coefficient of 0.72, an RMSE of 498.7 m, and a mean bias of −202.1 m. These errors are within the variability arising from differences in daytime PBLH-identification methodology of common techniques such as inversion height, parcel mixing, and index of refraction techniques (Seidel et al. 2010).

LCL is computed using the MetPy python package (May et al. 2022). MetPy accomplishes this by computing LCL dewpoint from the surface pressure. Then LCL pressure is computed using surface temperature and dewpoint. The computation is repeated using the new pressure, temperature, and dewpoint values until convergence is reached. The LFC is calculated as the first level at which a surface parcel lifted dry then moist adiabatically and possesses a temperature that is warmer than the environmental temperature and above the LCL. This is consistent with the definition provided in the *Glossary of Meteorology* (American Meteorological Society 2022).

f. Equivalent temperature

Further insight into the L-A interactions and influence of irrigation can be determined by using equivalent temperature T_E (Lachenmeier 2020), a measure best utilized for expressing

changes in heat content related to changes in moisture (i.e., moist enthalpy) (Pielke et al. 2004; Younger et al. 2019; Zhang et al. 2019). Equivalent temperature can be expressed as follows:

$$H = C_p T + L_v q, \tag{1}$$

where H is moist enthalpy (J Kg^{-1}), C_p is the isobaric specific heat of air (1005 J Kg^{-1} K^{-1}), T is air temperature (K), L_v is the latent heat of vaporization (2.5×10^6 J kg^{-1}) and q is specific humidity. Since mixing ratio is related to specific humidity (American Meteorological Society 2020), we have used the following expression to derive the latter:

$$q = r/(r + 1), \tag{2}$$

where r is the mixing ratio. Mixing ratio is calculated from vapor pressure of the air and atmospheric pressure where vapor pressure was calculated using Bolton's equation (Bolton 1980). To convert moist enthalpy into units of temperature (K), the following expression is used:

$$T_E = H/C_p. \tag{3}$$

the T_Es were then compared with observed air temperatures at the individual ISFS sites and later averaged over the six irrigated and six nonirrigated sites separately.

3. Results

a. *Near-surface air temperature and dewpoint temperature*

Utilizing observations at 5-min intervals, 30-min and daily averages were calculated (Lachenmeier 2020). Daily minimum and maximum values were also considered during the analysis. To understand changes in these variables linked to land use, averages from six locations over irrigated and six over nonirrigated were calculated (Figs. 2a,b). Air and dewpoint temperature analyses reveal notable differences in near-surface meteorological conditions over irrigated and nonirrigated land uses during the early growing season (IOP 1) and the peak growing season (IOP 2). Applications of t tests show that differences are statistically significant ($p < 0.05$) during IOP 2 for both air and dewpoint temperature.

During IOP 1, relative to over nonirrigated land use, average maximum air temperature was slightly higher (0.29°C) over irrigated areas. Subsequently, transition to increased irrigation started and resulting lowering of temperature over irrigated areas have begun during the inter-IOP period. As irrigation further increased, temperature was 0.60°C lower over irrigated land use than over nonirrigated land use for IOP 2 (Fig. 2a). This was due to the applications of irrigation resulting in higher latent and lower sensible heat fluxes (further discussion is provided in the following section) during the peak growth period of the plants (IOP 2).

Much like air temperature, the difference between dewpoint temperature over irrigated and nonirrigated croplands was small in the early growing season (IOP 1). Around the first week in July, when irrigation applications became more frequent, dewpoint temperatures at the irrigated sites were noticeably higher than the nonirrigated sites. It is found that average maximum dewpoint temperature over irrigated areas was 22.67°C, and for nonirrigated areas it was 21.57°C during IOP 2. Hence, it was 1.10°C higher over irrigated areas during IOP 2. Dewpoint temperature was 0.45°C lower over irrigated areas during IOP 1. Figure 2b depicts this midseason shift and elevated dewpoint temperatures over irrigated sites during IOP 2.

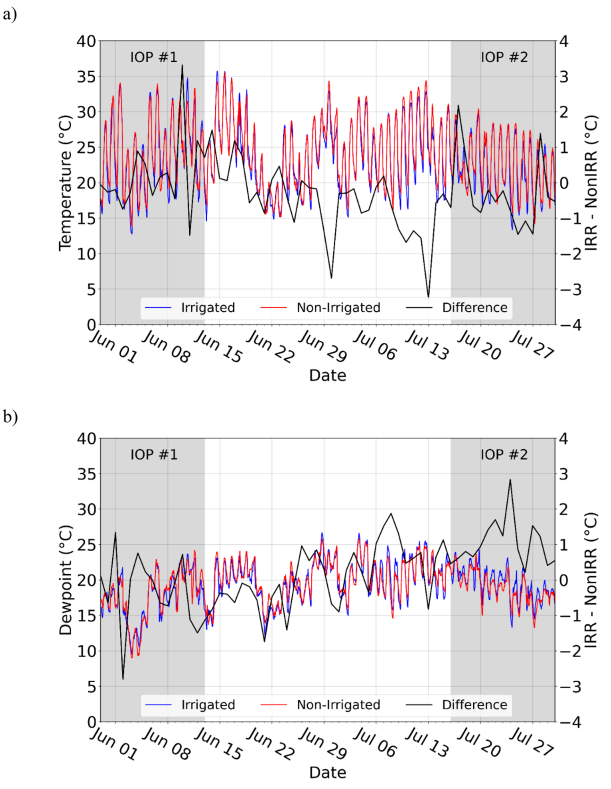

FIG. 2. Thirty-minute (a) air temperatures and (b) dewpoint temperatures averaged over the six irrigated and six nonirrigated sites during the growing season of 2018; temperature starts to decrease and dewpoint temperature starts to increase over irrigated areas around after 22 Jun as irrigation increases. Note that a comparison of irrigated and nonirrigated air temperatures during IOP 1 resulted in no statistical significance, but for IOP 2 comparisons resulted in statistically significant differences ($p < 0.05$). Limited irrigation during IOP 1 played an important role in this result. The same results apply for dewpoint temperature. The difference (irrigated minus nonirrigated) shown by the black line is the maximum from the irrigated sites minus the maximum from the nonirrigated sites for a given day.

b. *Heat flux*

During IOP 1 and 2, latent heat flux was greater than sensible heat flux over both irrigated and nonirrigated land uses. When daily averages for IOP 1 (Fig. 3a) and IOP 2 (Fig. 3b) were compared, a consistent difference between latent and sensible heat flux values was observed with latent heat fluxes dominating the daily averages. For IOP 1, higher values of

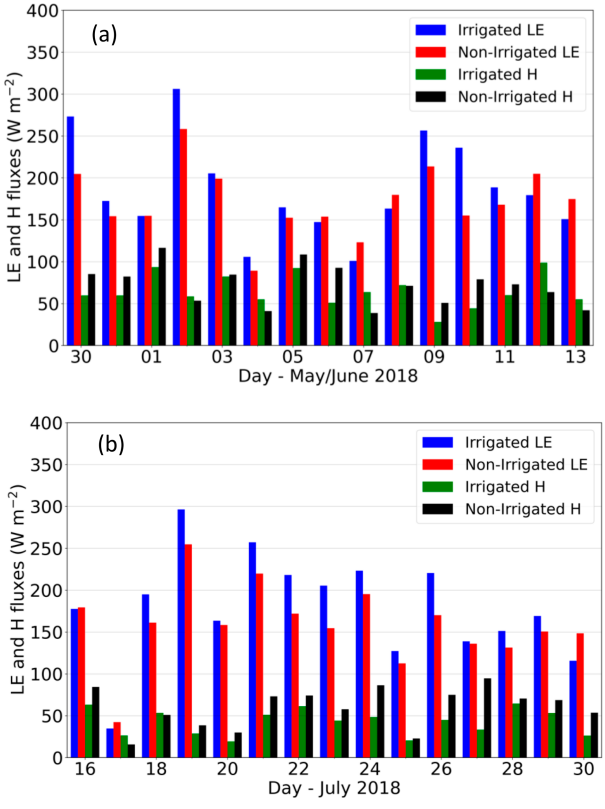

FIG. 3. Daytime (0500–1900 LST) average latent (LE) and sensible (H) heat flux for irrigated and nonirrigated sites during (a) IOP 1 and (b) IOP 2. For IOP 1 for irrigated and nonirrigated, LE is 187 and 172 W m^{-2}, respectively, and H is 65 and 72 W m^{-2}, respectively. For IOP 2 for irrigated and nonirrigated, LE is 180 and 159 W m^{-2}, respectively, and H is 43 and 60 W m^{-2}, respectively.

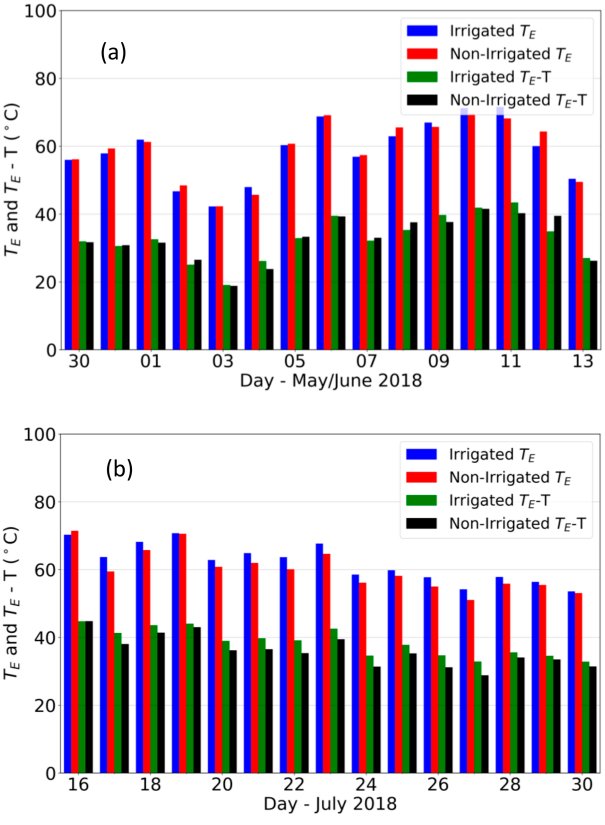

FIG. 4. Daytime (0500 to 1900 LST) average equivalent temperature T_E and air temperature difference $T_E - T$ for irrigated and nonirrigated sites during (a) IOP 1 and (b) IOP 2.

latent heat flux were associated with higher soil moisture linked to precipitation events, whose onset can be identified in the air temperature, dewpoint temperature, and soil moisture observations. Given the relatively wet conditions during the early growing season of 2018, the response observed on 2 June (Fig. 3a) was similar to the response produced from irrigation application days in IOP 2 (Fig. 3b). Therefore, in 2018, the early growing season latent heat flux was partly influenced by precipitation and resultant changes in soil moisture while during the peak growing season it was largely influenced by applications of irrigation (Rappin et al. 2022). Again, it is evident that both IOP 1 and IOP 2 produced higher latent heat flux while sensible heat flux was lower. During IOP 1, relative to over nonirrigated land use, latent heat flux was 15 W m^{-2} higher over irrigated areas and sensible heat flux was 7 W m^{-2} lower (Fig. 3a). Similar differences between irrigated and nonirrigated land use were observed during IOP 2. However, these differences were greater in magnitudes. Latent heat flux for irrigated areas was 20 W m^{-2} higher, on the average, than for nonirrigated areas while sensible heat flux was 17 W m^{-2} lower (Fig. 3b). Furthermore, 30-min data show statistically significant differences ($p < 0.05$) in fluxes between irrigated and nonirrigated land uses during IOP 2. These differences provide a clear indication of the changes in land–atmospheric interactions due to irrigation. In addition, a further summary of the data is provided in a Bowen ratio plot (see Fig. S1 in the online supplemental material).

c. T_E

It is indicated previously in the methodology section that T_E provides total heat content (dry + moist) of the atmosphere (Pielke et al. 2004; Younger et al. 2019). Hence, irrigation should increase atmospheric moisture and moist heat content, leading to an increase in total heat content (Zhang et al. 2019). The T_E, thus, provides an additional measure for understanding the impacts of irrigated land use (and land-use change) on the atmosphere. A comparison of T_E for irrigated and nonirrigated areas shows that differences during IOP 1 were negligible in the early growing season (Fig. 4a). Limited irrigation applications played a role in these small differences in T_E. During IOP 1, average daily T_E for irrigated sites was 58.78°C while 58.87°C was reported for nonirrigated sites. The highest T_E for irrigated sites was 71.55°C and for nonirrigated sites it was 69.45°C. In addition, the average T_E and air temperature difference ($T_E - T$) for irrigated sites was 32.80° and 32.77°C for nonirrigated, during IOP 1. Moreover, the largest

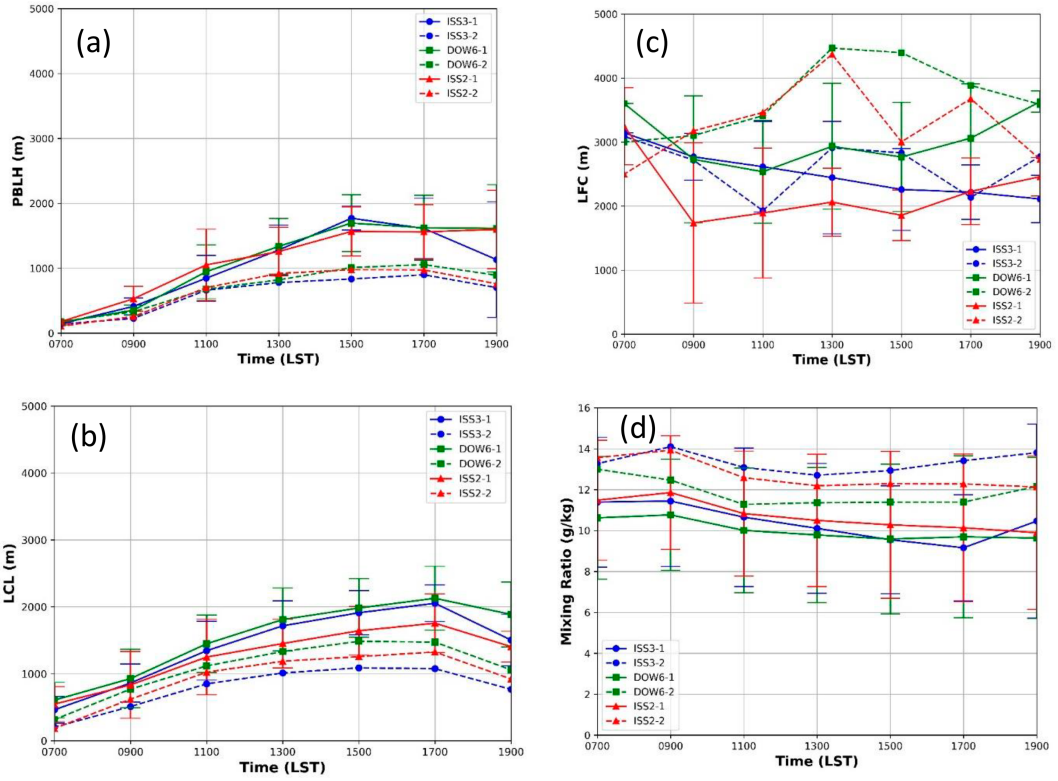

FIG. 5. Convective parameters, showing the full IOP average (a) PBLH, (b) LCL, (c) LFC, and (d) PBL w for irrigated York (ISS3), nonirrigated Rogers Farm (ISS2), and transitional land use (DOW6) at the respective radiosonde launch times. IOP 1 and 2 are indicated by 1 and 2, respectively, in the labels. Corresponding values are in Table 4. Whiskers show the 2-std-dev envelope for IOP 2. For clarity of the plots, whiskers are not added for IOP 1. LST = UTC − 6 h.

average daily difference between T_E and air temperature for irrigated sites was 43.39°C and, for nonirrigated sites it was 41.55°C. These differences essentially show contributions of moisture in T_E. As the growing season progressed and reached a key transitional point in late June/early July from less irrigation to consistently higher irrigation applications, a clearer increase in T_E was observed (Fig. 4b). Irrigated site averages were noticeably higher (on average $>$ 2°C) during IOP 2 than during IOP 1. Specifically, during IOP 2 average daily T_E for irrigated sites was 62.0°C, while for nonirrigated sites it was 59.97°C. Moreover, 30-min data show a statistically significant difference ($p < 0.05$) of T_E between irrigated and nonirrigated land uses during IOP 2. In addition, the average T_E and air temperature difference for irrigated and nonirrigated sites were 38.48° and 36.04°C, respectively, during IOP 2. In an earlier study, a mean of ~60°C T_E during the summer months was found in Kentucky (Younger et al. 2019). On average, T_E value over irrigated areas in eastern Nebraska was 62°C during IOP 2. Thus, due to irrigation and increased atmospheric moisture content, T_E in Nebraska was as high as in the east-central United States during similar time periods. The results from GRAINEX observations are also consistent with the findings that show increased T_E over irrigated locations in Kansas and Nebraska (Zhang et al. 2019).

d. *PBLH and LCL, LFC, and PBL mixing ratio for clear days*

Irrigation's impacts on PBLH (Seidel et al. 2010), LCL, LFC, and PBL mixing ratio r has not been well investigated in the past due to the unavailability of observational data. To determine the impacts, this study analyzed PBLH, LCL, LFC, and PBL r with radiosonde data from the three DOW and two ISS sites over irrigated and nonirrigated land cover (Figs. 5a–d). Clear and nonclear days can substantially impact PBL development and PBL development measures. As a result, first, we have identified clear and nonclear days for IOP 1 and 2 and then subsequently analyzed PBL development parameters for these two types of days for these two periods. This research selected the clear days based on visual inspection of satellite data from the NASA Worldview (NASA 2021). For this purpose, subhourly visible imagery from *GOES-16* was manually inspected for lack of cloud cover during hours of strong heating (~1000–1800 LST). Days with few to no clouds were accepted as clear days. Days with scattered fair-weather cumulus were accepted as clear days as well, in part due to the cumuli suggesting vigorous boundary layer mixing. This study selected five clear days during IOP 1 and four in IOP 2 (total 9 days). The remaining days (21 days) were considered as nonclear days. As indicated in the introduction, the IOPs were selected carefully to

TABLE 4. Clear-day average PBL heights (PBLH; m), lifting condensation level (LCL; m), level of free Cocection (LFC; m), and PBL mixing ratio (r; g kg^{-1}) for transitional DOW6, nonirrigated Rogers Farm, and irrigated York Airport during IOP 1 and IOP 2. Values correspond to Figs. 6a–d. The t test is used for statistical significance. Boldface roman and boldface italic type indicate that the difference between IOP 1 and 2 is statistically significant at $p < 0.1$ and $p < 0.05$, respectively. One and two asterisks indicate that the difference between irrigated and nonirrigated land use is statistically significant at $p < 0.1$ and $p < 0.05$, respectively.

		Transitional land use (DOW6)				Nonirrigated Rogers farm (ISS2)				Irrigated York (ISS3)			
Time	IOP	PBLH (m)	LCL (m)	LFC (m)	r (g kg^{-1})	PBLH (m)	LCL (m)	LFC (m)	r (g kg^{-1})	PBLH (m)	LCL (m)	LFC (m)	r (g kg^{-1})
0700 LST	IOP 1	168	607	***3602***	10.62	***177***	**547**	***3248*****	11.48	146	463	***3144*****	11.39
	IOP 2	180	316	***3001***	13.00	***109***	**184**	***2498*****	13.57	141	204	***3090*****	13.27
0900 LST	IOP 1	355	929	2730	10.77	***531***	834	1738	11.86	**413**	863	2770	11.44
	IOP 2	330	771	3102	12.47	***256***	621	3176	13.93	**228**	511	2718	14.10
1100 LST	IOP 1	947	1449	2537	10.01	1052	1250	1892*	10.83	846	1345	2616*	10.65
	IOP 2	680	1118	3414	11.28	702	1024	3463	12.58	662	850	1929	13.09
1300 LST	IOP 1	**1337**	1811	2934	9.78	1257	**1452***	***2063***	10.49	**1281**	**1717***	2445	10.11
	IOP 2	**821**	1333	4469	11.36	921	**1188***	***4372***	12.19	**781**	**1013***	2912	12.70
1500 LST	IOP 1	***1697***	**1983**	2767	9.59	***1568***	1643	1857	10.28	***1771***	***1912***	2260	**9.55**
	IOP 2	***1012***	**1486**	4397	11.39	***978****	1257	3004	12.29	***835****	***1089***	2832	**12.94**
1700 LST	IOP 1	***1623***	***2128***	3062	9.69	***1561***	1756	2231	10.13	***1613***	***2054***	2218	***9.16***
	IOP 2	***1056***	***1474***	3885	11.39	***975***	1326	3677	12.28**	***900***	***1077***	2136	***13.42*****
1900 LST	IOP 1	1615	***1887***	3631	9.63	1598	***1406***	2459*	9.90	1134	***1504***	2111*	10.46
	IOP 2	892	***1059***	3589	12.16	760	***922***	2732	12.13**	702	***768***	2775	13.81**
Mean	IOP 1	1106	1542	3038	10.01	1106	1270	2213	10.71	1029	1408	2509	10.39
	IOP 2	710	1080	3694	11.86	672	932	3275	12.71	607	787	2627	13.33

address the objectives of this research. In addition, large sampling of the atmosphere (1200 radiosonde launches in 30 days; 40 per day) ensured sufficient data representing various land surface and atmospheric conditions. This section of our paper focuses on clear days. The following section includes results for nonclear days.

1) PBLH

The average PBLH were calculated for clear days over irrigated and nonirrigated areas for IOP 1 and 2 using data from all radiosonde launches. The data were then plotted with respect to the deployment hours (Fig. 5a and Table 4). As shown in Fig. 1, ISS 2 was located within the nonirrigated area and ISS 3 was over irrigated land uses. Radiosondes also were launched from the mobile radar locations (DOW6, DOW7, and DOW8). DOW7 and 8 were located over nonirrigated and irrigated areas and DOW 6 along the transitional area of nonirrigated and irrigated land use (see Fig. 1). Radiosonde data from the DOW6-8 locations are analyzed but for brevity we present results from the DOW6 location. This provides an opportunity to present analysis from a range of land uses, from irrigated (ISS 3) to transitional (DOW 6) to nonirrigated (ISS 2).

We have focused on the morning [~0700 LST (~1300 UTC)] to late afternoon/evening transition period [~1900 LST (~0100 UTC)] when PBL development can be effectively captured by the radiosonde (Table 4). Note that there is a 6-h lag in LST relative to UTC, and hence LST = UTC − 6 h.

It is evident that PBLH was generally higher during IOP 1, as noted above. For example, over irrigated York, on average PBLH were 146, 413, 846, 1281, 1771, 1613, and 1134 for the 0700, 0900, 1100, 1300, 1500, 1700, and 1900 LST radiosonde launching times, respectively, during IOP 1 (Table 4; statistically significant differences are identified in the table). However, for IOP 2 they were 141, 228, 662, 781, 835, 900, and 702 m over irrigated land use for the same times. Average PBLH over nonirrigated Rogers Farm were 177, 531, 1052, 1257, 1568, 1561, and 1598 m for the same radiosonde launch times during IOP 1. The PBLH were 109, 256, 702, 921, 978, 975 and 760 m for the same launching times, during IOP 2. Similar results were found from transitional DOW6 (Table 4). Overall, the average daily PBLH was 1029 for IOP 1 while 607 m for IOP 2 under irrigated land use. It was 1106 m during IOP 1 and 671 m during IOP 2 for nonirrigated land use. There were 422 and 435 m lowering of the PBLH, respectively, over irrigated and nonirrigated land use from early to peak growing season.

Results from these radiosonde data analyses (Fig. 5a) indicate that PBLH during the early part of the growing season (IOP 1) was higher over irrigated, transitional, and nonirrigated land use when compared with the late growing season (IOP 2). Weatherwise, more active conditions and larger sensible heat flux (increased turbulence) led to deeper PBL during IOP 1, as was expected. For example, over irrigated areas and from 0500 to 1900 LST, average sensible heat flux during IOP 1 was 65 W m^{-2} and for IOP 2 it was 43 W m^{-2}. It was 72 and 60 W m^{-2} for the same two IOPs over nonirrigated land use. In addition, relative to the irrigated York and during IOP 1, the PBL grew faster (and PBLH remained higher) over nonirrigated Rogers Farm from 0700 to 1100 LST. We suggest higher sensible heat flux and relatively drier soil moisture conditions over the nonirrigated areas allowed such PBL growth during the early part of a day. In short, land use (irrigation and nonirrigation) played an important role in evolution of the boundary layer.

2) LCL

Analysis of data suggests that at the diurnal time scale, average LCL increased as the day progressed (Fig. 5b and Table 4). For example, at irrigated York average LCLs were 463, 863, 1345, 1717, 1912, 2054, and 1504 m at 0700, 0900, 1100, 1300, 1500, 1700, and 1900 LST, respectively (Fig. 7b and Table 1). Over nonirrigated Rogers Farm, average LCLs were 547, 834, 1250, 1452, 1643, 1756, and 1406 m for the same times (Fig. 6b and Table 4). In addition, it is also found that average LCLs were lower during IOP 2 than during IOP 1 over both irrigated and nonirrigated areas. Over irrigated York, during IOP 2, average LCLs were 204, 511, 850, 1013, 1089, 1077, and 768 m for the same radiosonde launching times, respectively (Fig. 6b and Table 4). Over Rogers Farm during IOP 2, LCLs for the same radiosonde launch times were 184, 621, 1024, 1188, 1257, 1326, and 922 m. The decrease of LCL increased probability of cloud formation over both irrigated and nonirrigated areas but more so over irrigated areas because of larger decrease. In addition, during IOP 2 the average LCL was 787 m over irrigated York and 932 m over nonirrigated Rogers Farm. Thus, relative to nonirrigated areas, on the average, LCL was 145 m lower over irrigated areas during IOP 2. This study also finds that the magnitude of the lowering of LCL during IOP 2 over irrigated areas was greater than over nonirrigated areas. Over irrigated York during IOP 2, on average, LCL was 621 m lower than during IOP 1. Over nonirrigated Rogers Farm, relative to IOP 1, LCL was 338 m lower during IOP 2. In short, the increased lowering of LCL over irrigated areas provides conditions that are more favorable for cloud formation relative to nonirrigated land use.

Radiosonde launching site DOW6 represents a transitional area from nonirrigated to irrigated land use. As a result, observations can potentially reflect impacts of both land uses. Overall, the LCL was higher relative to irrigated York and nonirrigated Rogers Farm for both IOPs (Fig. 6b and Table 4). The data also show that, like the other two locations/land uses and relative to IOP 1, the LCL was lower during IOP 2 (Fig. 6b and Table 4).

3) LFC

Analysis of radiosonde data suggests that during IOP 1, the LFC became lower with the progression of day and starts to increase toward the end of the day (Fig. 5c and Table 4). Relative to irrigated land use, LFCs were lower over nonirrigated land use. LFCs were notably higher over DOW 6. It is well known that the lowering of the LFC and reduction in LFC and LCL differences enhances the potential of convection. Observations show that LCL increases as the day progresses. Hence, the simultaneous lowering of LFC and increase

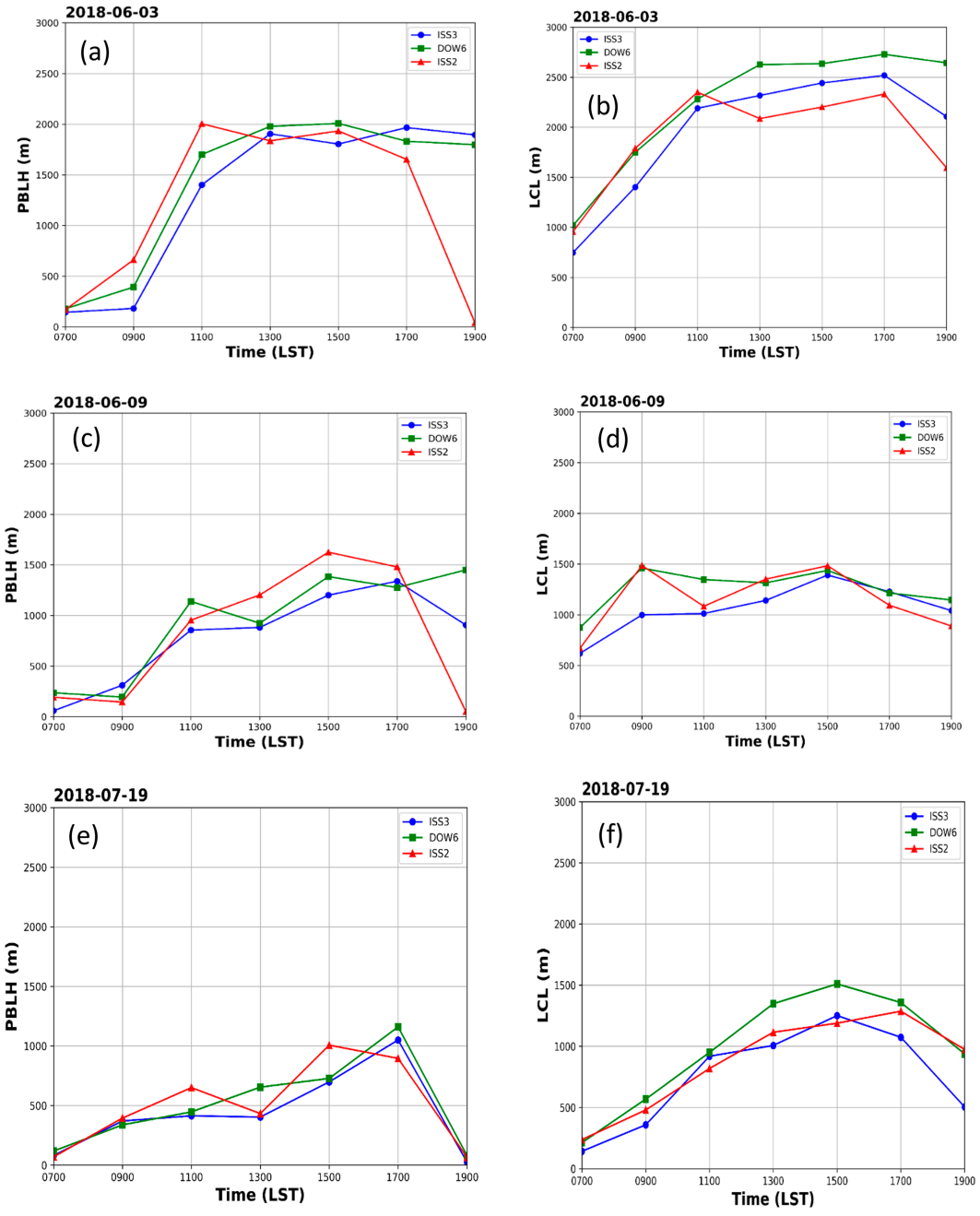

FIG. 6. Convective parameters for irrigated York (ISS3), nonirrigated Rogers Farm (ISS2), and transitional land use (DOW6): (left) PBLH and (right) LCL for (a),(b) 3 Jun (IOP 1); (c),(d) 9 Jun (IOP 1); and (e),(f) 19 Jul (IOP 2) 2018.

of LCL resulted in progressively smaller LFC and LCL differences, which enhance the potential for convective cloud development.

During IOP 1 average LFC-LCL differences were 1101 (the lowest), 943, and 1496 m over irrigated, nonirrigated, and transitional land uses, respectively. During IOP 2, these differences were 1840, 2342, 2614 m Moreover, on the average convection potentials were the highest over irrigated areas during IOP 2 (1840 m). On a diurnal scale, based on the lowest LFC-LCL (164 m), convective cloud development potential was highest at 1700 LST over irrigated areas during IOP 1. It was the highest also at 1700 LST during IOP 2 when LFC-LCL was 1059 m. Over nonirrigated land use this potential was highest at 1500 LST for both IOPs. The LFC-LCL difference was 214 m during IOP 1and 1747 m for IOP 2.

4) PBL MIXING RATIO

Available PBL moisture content such as mixing ratio r can notably impact LCL and LFC and hence convection initiation and cloud development. It is found that the average PBL was higher over irrigated land use than over both nonirrigated and transitional land uses during IOP 1 and IOP 2. The PBL r for early growing season over irrigated land use was 10.39 and increased to 13.33 g kg^{-1} during peak growing season (Fig. 5d and Table 4). They were 10.71 g kg^{-1} for the early and 12.71 g kg^{-1} during peak growing season for nonirrigated land use. It is clear that the increase over irrigated land use was greater during IOP 2 than over nonirrigated land use. During IOP 1 all three land uses show somewhat two diurnal peaks for PBL r, one in the morning and one during the afternoon–evening transition (Fig. 5d). However, for IOP 2 these dual peaks are discernable and demonstrate the impacts of irrigation and land use. In addition, these dual peaks of PBL r also occurred when PBLHs are at their lowest and conditions are very stable (Fig. 5a).

e. PBLH, LCL, LFC, and PBL mixing ratio for nonclear days

1) PBLH

Analogous to clear days, the PBLH was also higher during IOP 1 for nonclear days. For example, over irrigated York, on average PBLH heights were 124, 368, 723, 1025, 1193, 1120, and 961 for 0700, 0900, 1100, 1300, 1500, 1700, and 1900 LST radiosonde launching times, respectively, during IOP 1 (Table 5; statistically significant differences are identified in the table). However, during IOP 2 they were 160, 333, 586, 659, 687, 1021, and 453 m over irrigated land use for the same times. This clearly suggests that irrigation impacts on the lower troposphere are not limited only during clear days but also for other types of conditions. *It is an important finding and shows that land use and irrigation forcing can be sustained under nonclear days and observable when background atmospheric conditions are unstable.*

Observations from Rogers Farm and DOW6 demonstrate overall similar results (Table 5). For nonclear days, average daily PBLH was 788 m for IOP 1 while it was 557 m for IOP 2 under irrigated land use. They were 817 and 574 m for the for nonirrigated land use. Hence, there were 231 and 243 m reduction of PBLH over irrigated and nonirrigated land use, respectively.

2) LCL

For nonclear days, the LCL increased as the day progressed (Table 5), which is similar to clear days. Again, relative to IOP 1, it is found that the average LCL was lower during IOP 2, over both irrigated and nonirrigated areas. Average LCLs were 534 m for irrigated York and 610 m for nonirrigated Rogers Farm during IOP 2. Relative to IOP 1, LCLs were lowered to 681 and 550 m for irrigated York and nonirrigated Rogers Farm, respectively. Again, as during clear days, the

TABLE 5. As in Table 4, but for the nonclear-day average.

		Transitional land use (DOW6)				Nonirrigated Rogers farm (ISS2)				Irrigated York (ISS3)			
Time	IOP	PBLH (m)	LCL (m)	LFC (m)	r (g kg^{-1})	PBLH (m)	LCL (m)	LFC (m)	r (g kg^{-1})	PBLH (m)	LCL (m)	LFC (m)	r (g kg^{-1})
0700 LST	IOP 1	244	***664***	3897	11.84	160	***529***	***3636***	12.30	***124***	***459***	***3410***	12.66
	IOP 2	258	***256***	2967	11.97	143	***124***	***1015***	12.51	***160***	***165***	***1551***	12.57
0900 LST	IOP 1	297	***1134***	***3257***	11.85	397	***1011*****	2857	12.48	368	***837*****	2708	13.07
	IOP 2	241	***564***	***1988***	12.07	288	***440***	1849	12.81	333	***422***	1765	12.77
1100 LST	IOP 1	**911**	***1460***	***3168***	11.17	***886***	***1235***	***2399***	12.18	723	***1250***	***2684***	12.52
	IOP 2	**548**	***787***	***1813***	12.11	***499***	***657***	***1251***	12.84	586	***567***	***1017***	13.11
1300 LST	IOP 1	948	***1703***	***3406***	11.60	**1000**	***1299****	2047	12.15	***1025***	***1502****	***2993***	12.17
	IOP 2	1168	***923***	***1655***	11.78	***668***	***787***	1477	13.00	***659***	***639***	***1252***	13.60*
1500 LST	IOP 1	**1311**	***1954***	***3178***	11.28	**1123**	***1505*****	***2840***	11.88	***1193***	***1714*****	***2732***	**11.98**
	IOP 2	**794**	***889***	***1582***	12.96	***776***	***763***	***1366***	13.76	***687***	***709***	***1256***	**13.98**
1700 LST	IOP 1	1404	***1776***	***3182***	11.92	1223	***1472***	***2853***	12.39	1120	***1505***	***2976***	12.59
	IOP 2	1250	***1016***	***1693***	12.36	883	***859****	***1305***	13.81	1021	***714****	***1166****	13.63
1900 LST	IOP 1	1196	***1454***	***3797***	12.02	930	***1074*****	***3168***	12.41	***961***	***1242*****	***3642***	12.95
	IOP 2	945	***731***	***1485***	12.88	758	***642*****	***1053***	13.73	***453***	***524*****	***1558***	14.00
Mean	IOP 1	902	1449	3412	11.67	817	1161	2829	12.26	788	1216	3021	12.56
	IOP 2	743	738	1883	12.30	574	610	1331	13.21	557	534	1366	13.38

magnitude of the lowering of LCL during IOP 2 over irrigated areas was greater than over nonirrigated areas.

3) LFC

Analogous to clear days, the LFC became lower with the progression of day and particularly through midafternoon (Table 5). It is also found that while the LFC was lowered with the progression of day, the LCL was increased, and hence LFC and LCL differences were reduced and the potential for convection was increased. Again, relative to IOP 1, the LFC was reduced notably during IOP 2. On average, these reductions of LFCs were 1654, 1498, and 1529 m for irrigated York, nonirrigated Rogers Farm, and transitional DOW 6 locations, respectively. Again, irrigation impacts are obvious for nonclear days.

4) PBL MIXING RATIO

For nonclear days, the PBL r was largely higher over irrigated land use than over both nonirrigated and transitional land uses during IOP 1 and IOP 2 throughout the day. This is similar to diurnal changes in PBL r during clear days over these three land uses. On average, the PBL r for IOP 1 and IOP 2 over irrigated land use were 12.00 and 13.52 g kg^{-1}, respectively (Table 5). For nonirrigated land use, it was 12.56 g kg^{-1} for IOP 1 and increased to 13.38 g kg^{-1} for IOP 2. Again, it is evident that the increase over irrigated land use was greater during IOP 2 than over nonirrigated land use.

f. Results from the selected dates during early growing season (IOP 1)

To further understand and verify the overall findings presented in the previous sections and the influence of irrigated and nonirrigated land use, observations from several representative days were investigated (Figs. 6a–f). The objective is to assess whether irrigation and land-use impacts are identifiable for different parts of the growing season (early vs peak growing season) when crop condition and irrigation applications are dissimilar (relatively limited vs extensive irrigation) and background weather conditions were also different. Two dates were selected for IOP 1 and two for IOP 2. Dates chosen for IOP 1 include 3 June, when conditions were favorable for land–atmospheric interactions and 9 June, when convective activity impacted the entire study area.

1) IOP 1: 3 JUNE

On 3 June, the study region was dominated by high pressure and as a result, fair weather and clear skies were observed. Over a 3-day period, cooler air temperatures were observed around 3 June, which reflected in the climatological average as compared with the weeks preceding and following 3 June where 3°–6°C temperature departures were observed (NOAA 2020).

It is found that weather conditions were favorable for relatively high PBLH (up to 2004 m). In comparison with irrigated York, the rapid growth of PBL over nonirrigated Rogers Farm with sunrise and similar rapid collapse during the afternoon (Fig. 6a) is linked to relatively drier land surface conditions as observed in the soil moisture data (not shown). This suggests slower development of the PBL over irrigated areas for 3 June when land surface was wet. The LCL shows comparable results where it remained lower over irrigated York than over nonirrigated Rogers Farm, during the early part of the day (Fig. 6b). However, along with PBL, LCL rapidly lowered over nonirrigated and drier Rogers Farm during the afternoon–evening transition.

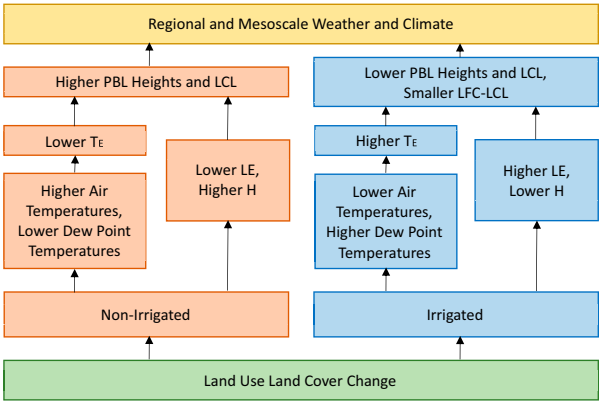

FIG. 7. A simplified conceptual model of the impacts of irrigated and nonirrigated land use. Note that albedo is lower over irrigated land use.

2) IOP 1: 9 JUNE

An afternoon mesoscale convective system formed over southern South Dakota and central Nebraska on 8 June and propagated east to the GRAINEX study area during the early morning of 9 June. This event produced heavy rain. Larger differences of average air temperature between irrigated and nonirrigated sites were observed (approximately 3°C) with air temperatures over the irrigated region being higher than the nonirrigated (Figs. 2a,b). This difference is likely associated with the west to east propagation of the storm and the delayed early morning heating of the eastern sites (nonirrigated) due to residual cloud cover.

The highest height of the PBL was 1625 m, while for LCL it was 1484 m (Figs. 6c,d) and thus lower than those on 3 June. It is also observed, relative to Rogers Farm, that PBLH remains lower over irrigated York for most of the day. For example, during midafternoon (1300 LST) PBLH over irrigated York and nonirrigated Rogers Farm were 882 and 1203 m, respectively. Again, over nonirrigated Rogers Farm, PBLH and LCL declined more rapidly during the afternoon–evening transition. During the last radiosonde launch (1900 LST), PBLH over irrigated York was 906 m and over nonirrigated Rogers Farm it was 50 m.

g. Results from the selected dates during peak growing season (IOP 2)

The number of precipitation events were notably less during the second half of the growing season (including IOP 2), resulting in increased irrigation. As noted before, two dates were chosen for IOP 2 for further analysis. These dates

include 19 July, which exhibited an early morning severe weather event with heavy precipitation simultaneously impacting irrigated and nonirrigated portions of the GRAINEX study area starting around 0600 UTC (0100 LT), and 22 July, which was a clear day.

1) IOP 2: 19 JULY

On this day, latent heat flux was higher over the irrigated and sensible heat flux was higher over nonirrigated sites (Fig. 4b; bars for 19 July). Due to the launches between sunrise and sunset, radiosondes were unable to capture the immediate impacts from the early morning precipitation. However, the soundings indicated slow PBL development for most of the day. Over irrigated land use, PBLH remained below 699 m through 1500 LST, while it was 1007 m over nonirrigated land use (Fig. 6e). These heights are lower when compared with soundings from 3 and 9 June of IOP 1 (Fig. 7a). Observations also suggest that PBLH and LCL for 19 July lacked a rapid increase (e.g., like 9 or 3 June) (Figs. 6a–f). These differences were especially noticeable between late morning through late afternoon. We suggest that this difference was due to land use and the availability of higher moisture over irrigated land use and lower moisture over nonirrigated land use.

2) IOP 2: 22 JULY

Conditions on 22 July were dominated by high pressure, with relatively clear skies following the dissipation of early morning fog. Air and dewpoint temperatures were slightly lower and higher over irrigated land uses than over nonirrigated land uses, respectively. Daily average latent heat fluxes over both irrigated and nonirrigated sites were higher than sensible heat fluxes. However, latent flux over irrigated land use (296 W m^{-2}) was noticeably higher than over nonirrigated land use (254 W m^{-2}). PBLH remained lower than 1000 m over all locations and it is further reduced over irrigated land use relative to the nonirrigated and transitional land uses. LCL also shows similar results and remained below 1500 m, which is further decreased relative to the IOP 1 days (up to ~2500 m).

4. Discussion

The results demonstrate that LULCC and irrigation impacts energy partitioning (latent and sensible heat flux), various near-surface meteorological variables (air temperature, dewpoint temperature, and equivalent temperature), evolution of the planetary boundary layer (PBLH changes), convective environment and their measures (LCL, LFC, and PBL mixing ratio). These changes are magnified under irrigated conditions and are complex. In addition, this study finds that differences in observations between irrigated and nonirrigated areas are further amplified in the latter half of the growing season. The average maximum air temperature over irrigated areas was 2.74°C lower during the peak growing season (IOP 2) than during the early part of the growing season (IOP 1), while average dewpoint temperature was 1.10°C higher during IOP 2. In addition, the difference between average irrigated and nonirrigated latent and sensible heat fluxes during IOP 1 were 15 and 7 W m^{-2}, respectively. During IOP 2, these differences were 20 and 17 W m^{-2}. Over irrigated areas, latent heat flux was larger and sensible heat flux smaller than over nonirrigated areas. This difference illustrates the partitioning of energy associated with additional moisture over irrigated areas. The availability of additional water via irrigation allows for increased latent heat flux, which resulted in the lowering of maximum air temperature. Irrigation also leads to higher near-surface atmospheric humidity and dewpoint temperature.

These results are consistent with previous findings that showed a decrease in maximum temperature over irrigated areas. For example, in a modeling study, Adegoke et al. (2003) found 1.2°C cooling of temperature over irrigated areas in Nebraska. In several observed climatological databased studies Mahmood et al. (2004, 2006, 2013) found a cooling trend and up to 1.01°C cooling of mean maximum temperature during the twentieth-century growing season over irrigated areas in comparison with nonirrigated land use in the Great Plains. Bonfils and Lobell (2007) also investigated impacts of irrigation on temperature and found ~0.2°C $decade^{-1}$ cooling trends in temperature during second half of the twentieth century and growing season in Nebraska.

A series of studies on the impacts of irrigation in California also reported overall cooling and a cooling trend of temperature (Christy et al. 2006; Bonfils and Lobell 2007; Kueppers et al. 2007, 2008; Sorooshian et al. 2014). For example, based on an observational databased study, Christy et al. (2006) found a 0.26°C $decade^{-1}$ cooling of growing season maximum temperature due to irrigation. In addition, several model-based studies estimated up to 7.5°C cooling of growing season maximum temperature in California. These studies also suggest that increases in latent heat flux due to irrigation resulted in the lowering of maximum temperature. In addition, from an observational databased research, Sen Roy et al. (2007) found up to 0.34°C lowering of growing season maximum temperatures over irrigated areas in India. They have also reported up to 0.53°C cooling of during individual growing season months. Their modeled-based assessment also shows an increase in latent heat flux over irrigated areas. In summary, findings from the GRAINEX are in agreement with the previous climatological and model-based studies. In addition, in this research we have directly demonstrated observed changes in fluxes over irrigated areas and their impacts on the lowering of maximum temperature.

As expected, T_E values were somewhat similar at irrigated and nonirrigated sites during the early growing season (IOP 1), but higher over irrigated areas during the peak growing season (IOP 2). For example, average T_E differences between irrigated and nonirrigated sites were 0.11°C during IOP 1 and 2.03°C during IOP 2. Since moisture notably influences T_E, higher T_E over irrigated areas suggests higher moisture contribution as compared with the nonirrigated T_E values in IOP 2 (Pielke et al. 2004). These results are consistent with previous findings by Younger et al. (2019), Zhang et al. (2019), and Na-Yemeh et al. (2020). Based on the analysis of climatological data from Nebraska and Kansas, Zhang et al. (2019) found

that T_E was notably higher over irrigated land use than over grasslands (i.e., nonirrigated) during the growing season. Younger et al. (2019) investigated mesoscale T_E in Kentucky using the Kentucky Mesonet (Mahmood et al. 2019) data and found that moist atmosphere leads to higher T_E relative to drier conditions. In follow-up research by Na-Yemeh et al. (2020), moist air masses have higher T_E than do dry air masses, and it peaks during peak growing season. These results, again, further support the findings of this paper.

Recently, Matthews et al. (2022) highlighted the importance of T_E and accounting of latent heat and atmospheric moisture in relation to weather and climate extremes. They have also demonstrated that climate change and related changes in heat content can be better tracked with the use of T_E. Matthews et al. (2022) noted that it is possible to have declining air temperature (accounts for dry heat content, dry-bulb temperature) while total heat content continues (dry and moist heat) increase. The result presented here, based on GRAINEX data, also clearly shows that while air temperature was decreased due to irrigation during peak growth phase (IOP 2), T_E (i.e., total heat content) increased. This study, potentially for the first time and from simultaneous observations shows linkages among increased latent heat flux, decreased air temperature, and increased atmospheric heat content (via T_E) over irrigated areas. Hence, irrigation and other forms of LULCC can and will continue to modify atmospheric heat content locally, regionally, and beyond. These changes need to be appropriately recognized and addressed.

To understand lower-tropospheric response to irrigation, data from the radiosonde launches (~1200) at the three DOW locations, nonirrigated Rogers Farm and irrigated York were also analyzed. The sounding data were used to complete LCL, LFC, and PBLH calculations. The analyses show the higher PBLH during IOP 1 for both irrigated and nonirrigated land uses, associated with larger sensible heat and increased turbulence. On the other hand, lower PBLH was observed during IOP 2, associated with plant growth and resultant increased latent heat flux. Increased applications of irrigation due to higher plant-water demand, and resultant increased latent heat flux led to an LFC with a tendency for lower heights over irrigated areas.

Lower PBLH and LCL also provide increased potential for cloud development and convective initiation. These observations also apply for the dates impacted by early morning convective precipitation. Overall, irrigated areas experienced higher latent heat flux, lower PBLH, LCL, LFC, and higher mixing ratio. These findings suggest that irrigation impacts on the PBL and associated convective conditions were sustained and continuous for varied land surfaces and land covers (early vs peak growing season) and weather conditions.

Results demonstrate connectivity between surface fluxes and planetary boundary layer development and stability linked to moist land surface conditions (Pielke et al. 2007; Eltahir and Pal 1996; Eltahir 1998; Findell and Eltahir 1999; Betts 2007; Winchester et al. 2017). It is well known that vegetation (in this case irrigated agriculture) has a strong influence on the distribution of surface fluxes and moisture, which directly impacts PBL development and PBLH (Winchester et al. 2017; Mahmood et al. 2011; Nair et al. 2011). Higher sensible heat flux produces more turbulence and thus increases PBLH. Higher latent heat flux has an opposite impact (shallow PBL/lower PBLH), which is observed over irrigated areas.

In a study focusing on vegetation–atmosphere interactions in the eastern United States, Freedman et al. (2001) found that PBLH peaked and subsequently lowered before and after the commencement of the growing season. The lowering of PBLH was linked to increased latent heat flux. The observations from GRAINEX agree with the findings by Freedman et al. (2001) and also show that higher latent heat flux from irrigated land use further increased the lowering of PBL and thus PBLH. Subsequent research by Mahmood et al. (2011) shows that vegetation cover and soil moisture play important roles in modulating height of the PBL with higher soil moisture resulting in lower PBLH in the east-central United States. They have also linked this response with the magnitude of latent heat flux where higher latent flux resulting in lower PBLH. Lawston et al. (2020) investigated impacts of irrigation in the Columbia River Basin in the northwestern United States. Their study reported that irrigation impacts PBLH and results in lower PBLH. In another study focusing on irrigated areas of Nebraska and Kansas, they found that irrigation resulted in lower PBLH. They have noted that as evaporative fraction [ratio of latent heat flux and (latent + sensible heat flux)] increases PBLH also lowers (Lawston et al. 2015).

In summary, findings from GRAINEX regarding the response of the PBLH over irrigated areas are consistent with results from other studies demonstrating its lowering with land surface and lower atmospheric moistening through other process (e.g., spring moistening due to increased latent heat flux). It is also evident that the impacts are "universal" regardless of geographic location. The result from the present study also clearly shows further lowering of PBLH from IOP 1 to IOP 2 as irrigation increased rapidly with increased crop-water demand. In addition, it is found that regardless of clear or nonclear days, irrigation lowers the PBLH.

Furthermore, previous research demonstrated that moist land surface condition allows higher physical evaporation and transpiration leading to higher atmospheric humidity and lower LCL (Betts 2007). It was also reported that lower LCL is associated with higher precipitation (Betts 2007). Smaller difference in LFC and LCL is also an indication of a favorable condition for convection (Bech et al. 2011; Alter et al. 2015; Chakraborty et al. 2018). Alter et al. (2015) succinctly discussed increased latent heat flux (and hence higher ET) leads to more moist PBL and lowering of LCL, thus providing an easier pathway for cloud formation. It is also noted that if LCL is lowered too much and the depth between LCL and LFC increases then that condition may inhibit clouds from reaching LFC.

As noted previously, we have found in this study that the depth between LFC and LCL declined during midmorning and early afternoon and thus enhanced potential for convection and precipitation. These observational databased findings are in agreement with previous modeling studies (e.g., Qian et al. 2013; Huber et al. 2014) that show lowering of LCL and

LFC over the irrigated areas. In short, this observational data-based study confirms our conceptual and theoretical understanding of potential impacts of moist environment (in this case irrigation) on the PBL and lower atmospheric convective environment.

Figure 7 succinctly summarizes LULCC, irrigation (and nonirrigation), and linkages among various processes. It is clear that irrigation impacts mesoscale and near-surface atmospheric temperature, atmospheric and soil moisture, and atmospheric heat content. We suggest that some of these changes can also be observed on the regional scale. In addition, the results suggest that irrigation impacts mesoscale convective environment regardless of background atmospheric condition and it is reflected in changes in PBLH, LCL, LFC, and PBL moisture content. These changes should also impact mesoscale cloud development and timing of cloud development.

Furthermore, results indicate that irrigation changes mesoscale precipitation. For example, it is found in our previous study that a precipitation event developed and was sustained over irrigated area and then dissipated over nonirrigated area (Rappin et al. 2021; Fig. 8). A modeling study has been completed (Whitesel et al. 2024) for this event and results suggest that irrigation indeed impacted precipitation. Currently, additional modeling work is under way. For the assessment of irrigation impacts on regional scale precipitation, new modeling work is needed and currently under planning. However, in the meantime, we draw upon modeling research completed by DeAngelis et al. (2010), Harding and Snyder (2012a,b), and Huber et al. (2014). The results from these studies suggest that irrigation caused changes in downstream precipitation.

5. Final remarks

Novelty of the research can be found in the following:

- This study, for the first time, used extensive observational data to understand the impacts of irrigation on the planetary boundary layer atmosphere and convective environment throughout the growing season. These observations include surface fluxes and bihourly radiosonde launches, among others.
- The GRAINEX observations allowed us, for the first time, to investigate diurnal evolution of the lower troposphere under irrigated condition. The vast majority of the previous work used modeled data to investigate the impacts of irrigation on the lower troposphere. Here, with observations, we demonstrated and confirmed the impacts of irrigation.
- This research, for the first time, evaluated the impacts of adjacent irrigated versus nonirrigated land uses on the lower troposphere using observed data, where nonirrigated land use transitioned to irrigated. Remarkably, it was found that the lower troposphere responded differently under these two different adjacent land uses (~100 km × 100 km area) while under generally similar atmospheric influence.
- For the first time, results show changes in diurnal PBL evolution and convective environment as the season progressed and as irrigation applications increased due to higher crop-water demand. In other words, this study identified intraseasonal variations of irrigation and their impacts on near-surface atmosphere and convective environment.
- This research also shows that irrigation influences the convective environment regardless of background atmospheric condition.

Results of this study have implications in both weather forecasting and climate research. The findings that irrigation impacts the convective environment can be integrated into local and regional weather forecasting rubrics. They can potentially help to improve lead time for certain local and regional conditions. These include the timing of cloud development, diurnal variations of atmospheric humidity and heat content, moist heat stress, and human and animal comfort, among others.

As irrigation has been continually expanding over many regions of the world because of demand for food, irrigation and irrigation-driven LULCC and their impacts on climate need to be further investigated. It is evident from this study that there are seasonal-scale impacts of irrigation on the atmosphere as its applications modulate due to changes in crop-water demand linked to crop growth. In other words, the ramification of such changes in irrigation water applications in local, regional, and continental-scale climate needs to be assessed. These investigations should include downstream impacts of irrigation as well. We suggest that the results presented here are new and important and can be applicable for other parts of the world. As a result, it is necessary that efforts should be ongoing and well coordinated to determine current and future impacts of irrigation on weather and climate (Loveland and Mahmood 2014; Mahmood et al. 2016; McDermid et al. 2021). The results suggests that the future land-use policy recommendation development process should actively include potential impacts of irrigation, in the context of LULCC, on climate to minimize the unintended consequences of adoption of any particular polices.

Acknowledgments. The authors thank three anonymous reviewers for their valuable feedback, which helped to improve this paper. This research is funded by NSF Grants AGS-1853390 (authors Rezaul Mahmood and Eric Rappin), AGS-1720477 (author Udaysankar Nair), and AGS-1552487 (author Roger Pielke Sr.). The National Center for Atmospheric Research is sponsored by the National Science Foundation.

Data availability statement. All data used during this study are openly available from the NCAR/UCAR Earth Observing Laboratory (https://www.eol.ucar.edu/field_projects/grainex) as cited in Rappin et al. (2021).

REFERENCES

Adegoke, J. O., R. A. Pielke Sr., J. Eastman, R. Mahmood, and K. G. Hubbard, 2003: Impact of irrigation on midsummer surface fluxes and temperature under dry synoptic conditions: A regional atmospheric model study of the U.S. High Plains. *Mon. Wea. Rev.*, **131**, 556–564, https://doi.org/10.1175/1520-0493(2003)131<0556:IOIOMS>2.0.CO;2.

Ajaz, A., S. Datta, and S. Stoodley, 2020: High Plains Aquifer—State of affairs of irrigated agriculture and role of irrigation in the sustainability paradigm. *Sustainability*, **12**, 3714, https://doi.org/10.3390/su12093714.

Alter, R. E., Y. Fan, B. R. Linter, and C. P. Weaver, 2015: Observational evidence that Great Plains irrigation has enhanced summer precipitation intensity and totals in the midwestern United States. *J. Hydrometeor.*, **16**, 1717–1735, https://doi.org/10.1175/JHM-D-14-0115.1.

——, H. C. Douglas, J. M. Winter, and E. A. B. Eltahir, 2018: Twentieth century regional climate change during the summer in the central United States attributed to agricultural intensification. *Geophys. Res. Lett.*, **45**, 1586–1594, https://doi.org/10.1002/2017GL075604.

American Meteorological Society, 2020: Specific humidity. Glossary of Meteorology, https://glossary.ametsoc.org/wiki/Specific_humidity.

——, 2022: Level of free convection. Glossary of Meteorology, https://glossary.ametsoc.org/wiki/Level_of_free_convection.

Bala, G., K. Caldeira, M. Wickett, T. J. Phillips, D. B. Lobell, C. Delire, and A. Mirin, 2007: Combined climate and carbon-cycle effects of large-scale deforestation. *Proc. Natl. Acad. Sci. USA*, **104**, 6550–6555, https://doi.org/10.1073/pnas.0608998104.

Bech, J., and Coauthors, 2011: A Mediterranean nocturnal heavy rainfall and tornadic event. Part I: Overview, damage survey and radar analysis. *Atmos. Res.*, **100**, 621–637, https://doi.org/10.1016/j.atmosres.2010.12.024.

Betts, A. K., 2007: Coupling of water vapor convergence, clouds, precipitation, and land-surface processes. *J. Geophys. Res.*, **112**, D10108, https://doi.org/10.1029/2006JD008191.

Bolton, D., 1980: The computation of equivalent potential temperature. *Mon. Wea. Rev.*, **108**, 1046–1053, https://doi.org/10.1175/1520-0493(1980)108<1046:TCOEPT>2.0.CO;2.

Bonfils, C., and D. Lobell, 2007: Empirical evidence for a recent slowdown in irrigation-induced cooling. *Proc. Natl. Acad. Sci. USA*, **104**, 13 582–13 587, https://doi.org/10.1073/pnas.0700144104.

Brown, J. F., and M. S. Pervez, 2014: Merging remote sensing data and national agricultural statistics to model change in irrigated agriculture. *Agric. Syst.*, **127**, 28–40, https://doi.org/10.1016/j.agsy.2014.01.004.

Chakraborty, R., G. Basha, and M. V. Ratnam, 2018: Diurnal and long-term variation of instability indices over a tropical region in India. *Atmos. Res.*, **207**, 145–154, https://doi.org/10.1016/j.atmosres.2018.03.012.

Christy, J. R., W. B. Norris, K. Redmond, and K. P. Gallo, 2006: Methodology and results of calculating central California surface temperature trends: Evidence of human-induced climate change? *J. Climate*, **19**, 548–563, https://doi.org/10.1175/JCLI3627.1.

DeAngelis, A., F. Dominguez, Y. Fan, A. Robock, M. D. Kustu, and D. Robinson, 2010: Evidence of enhanced precipitation due to irrigation over the Great Plains of the United States. *J. Geophys. Res.*, **115**, D15115, https://doi.org/10.1029/2010JD013892.

Diffenbaugh, N. S., 2009: Influence of modern land cover on the climate of the United States. *Climate Dyn.*, **33**, 945–958, https://doi.org/10.1007/s00382-009-0566-z.

Eltahir, E. A. B., 1998: A soil moisture–rainfall feedback mechanism: 1. Theory and observations. *Water Resour. Res.*, **34**, 765–776, https://doi.org/10.1029/97WR03499.

——, and J. S. Pal, 1996: Relationship between surface conditions and subsequent rainfall in convective storms. *J. Geophys. Res.*, **101**, 26 237–26 245, https://doi.org/10.1029/96JD01380.

Findell, K. L., and E. A. B. Eltahir, 1999: Analysis of the pathways relating soil moisture and subsequent rainfall in Illinois. *J. Geophys. Res.*, **104**, 31 565–31 574, https://doi.org/10.1029/1999JD900757.

Freedman, J. M., D. R. Fitzjarrald, K. E. Moore, and R. K. Sakai, 2001: Boundary layer clouds and vegetation–atmosphere feedbacks. *J. Climate*, **14**, 180–197, https://doi.org/10.1175/1520-0442(2001)013<0180:BLCAVA>2.0.CO;2.

Gameda, S., B. Qian, C. A. Campbell, and R. L. Desjardins, 2007: Climatic trends associated with summerfallow in the Canadian prairies. *Agric. For. Meteor.*, **142**, 170–185, https://doi.org/10.1016/j.agrformet.2006.03.026.

Gullison, R. E., and Coauthors, 2007: Tropical forests and climate policy. *Science*, **316**, 985–986, https://doi.org/10.1126/science.1136163.

Harding, K. J., and P. K. Snyder, 2012a: Modeling the atmospheric response to irrigation in the Great Plains. Part I: General impacts on precipitation and the energy budget. *J. Hydrometeor.*, **13**, 1667–1686, https://doi.org/10.1175/JHM-D-11-098.1.

——, and ——, 2012b: Modeling the atmospheric response to irrigation in the Great Plains. Part II: The precipitation of irrigated water and changes in precipitation recycling. *J. Hydrometeor.*, **13**, 1687–1703, https://doi.org/10.1175/JHM-D-11-099.1.

He, Y., E. Lee, and J. S. Mankin, 2020: Seasonal tropospheric cooling in northeast China associated with cropland expansion. *Environ. Res. Lett.*, **15**, 034032, https://doi.org/10.1088/1748-9326/ab6616.

Huber, D. B., D. B. Mechem, and N. A. Brunsell, 2014: The effects of Great Plains irrigation on the surface energy balance, regional circulation, and precipitation. *Climate*, **2**, 103–128, https://doi.org/10.3390/cli2020103.

IPCC, 2019: Technical summary. *Climate Change and Land*, P. R. Shukla et al., Eds., Cambridge University Press, 37–74, https://doi.org/10.1017/9781009157988.002.

Kang, S.-L., and G. H. Bryan, 2011: A large-eddy simulation study of moist convection initiation over heterogeneous surface fluxes. *Bull. Amer. Meteor. Soc.*, **139**, 2901–2917, https://doi.org/10.1175/MWR-D-10-05037.1.

Kueppers, L. M., M. A. Snyder, and L. C. Sloan, 2007: Irrigation cooling effect: Regional climate forcing by land-use change. *Geophys. Res. Lett.*, **34**, L03703, https://doi.org/10.1029/2006GL028679.

——, and Coauthors, 2008: Seasonal temperature responses to land-use change in the western United States. *Global Planet. Change*, **60**, 250–264, https://doi.org/10.1016/j.gloplacha.2007.03.005.

Kuttippurath, J., and Coauthors, 2021: Observed rainfall changes in the past century (1901–2019) over the wettest place on Earth. *Environ. Res. Lett.*, **16**, 024018, https://doi.org/10.1088/1748-9326/abcf78.

Lachenmeier, E. J., 2020: Impacts of irrigated agriculture on the near surface and planetary boundary layer atmosphere: Results from the Great Plains Irrigation Experiment (GRAINEX). M.S. thesis, School of Natural Resources, University of Nebraska–Lincoln, 112 pp., https://digitalcommons.unl.edu/natresdiss/325/.

Lawston, P. M., J. A. Santanello Jr., B. F. Zaitchik, and M. Rodell, 2015: Impact of irrigation methods on land surface model spinup and initialization of WRF forecasts. *J. Hydrometeor.*, **16**, 1135–1154, https://doi.org/10.1175/JHM-D-14-0203.1.

——, J. A. Santanello, B. Hanson, and K. Arsensault, 2020: Impacts of irrigation on summertime temperatures in the Pacific

Northwest. *Earth Interact.*, **24**, https://doi.org/10.1175/EI-D-19-0015.1.

Lobell, D., G. Bala, A. Mirin, T. Phillips, R. Maxwell, and D. Rotman, 2009: Regional differences in the influence of irrigation on climate. *J. Climate*, **22**, 2248–2255, https://doi.org/10.1175/2008JCLI2703.1.

Loveland, T. R., and R. Mahmood, 2014: A design for a sustained assessment of climate forcing and feedbacks related to land use and land cover change. *Bull. Amer. Meteor. Soc.*, **95**, 1563–1572, https://doi.org/10.1175/BAMS-D-12-00208.1.

Maeda, E. E., T. A. Aberaa, M. Siljandera, L. E. O. C. Aragão, Y. M. de Moura, and J. Heiskanen, 2021: Large-scale commodity agriculture exacerbates the climatic impacts of Amazonian deforestation. *Proc. Natl. Acad. Sci. USA*, **118**, e2023787118, https://doi.org/10.1073/pnas.2023787118.

Mahmood, R., and K. G. Hubbard, 2002: Anthropogenic land-use change in the North American tall grass-short grass transition and modification of near-surface hydrologic cycle. *Climate Res.*, **21**, 83–90, https://doi.org/10.3354/cr021083.

——, ——, and C. Carlson, 2004: Modification of growing-season surface temperature records in the northern Great Plains due to land-use transformation: Verification of modelling results and implication for global climate change. *Int. J. Climatol.*, **24**, 311–327, https://doi.org/10.1002/joc.992.

——, S. A. Foster, T. Keeling, K. G. Hubbard, C. Carlson, and R. Leeper, 2006: Impacts of irrigation on 20th century temperature in the northern Great Plains. *Global Planet. Change*, **54**, 1–18, https://doi.org/10.1016/j.gloplacha.2005.10.004.

——, R. Leeper, and A. I. Quintanar, 2011: Sensitivity of planetary boundary layer atmosphere to historical and future changes of land use/land cover, vegetation fraction, and soil moisture in western Kentucky, USA. *Global Planet. Change*, **78**, 36–53, https://doi.org/10.1016/j.gloplacha.2011.05.007.

——, T. Keeling, S. A. Foster, and K. G. Hubbard, 2013: Did irrigation impact 20th century air temperature in the High Plains aquifer region? *Appl. Geogr.*, **38**, 11–21, https://doi.org/10.1016/j.apgeog.2012.11.002.

——, and Coauthors, 2014: Land cover changes and their biogeophysical effects on climate. *Int. J. Climatol.*, **34**, 929–953, https://doi.org/10.1002/joc.3736.

——, R. A. Pielke Sr., and C. A. McAlpine, 2016: Climate-relevant land use and land cover change policies. *Bull. Amer. Meteor. Soc.*, **97**, 195–202, https://doi.org/10.1175/BAMS-D-14-00221.1.

——, M. Schargorodski, S. Foster, and A. Quilligan, 2019: A technical overview of the Kentucky Mesonet. *J. Atmos. Oceanic Technol.*, **36**, 1753–1771, https://doi.org/10.1175/JTECH-D-18-0198.1.

Matthews, T., M. Byrne, R. Horton, C. Murphy, R. Pielke Sr., C. Raymond, P. Thorne, and R. L. Wilby, 2022: Latent heat must be visible in climate communications. *Wiley Interdiscip. Rev.: Climate Change*, **e779**, https://doi.org/10.1002/wcc.779.

May, R. M., and Coauthors, 2022: MetPy: A meteorological Python library for data analysis and visualization. *Bull. Amer. Meteor. Soc.*, **103**, E2273–E2284, https://doi.org/10.1175/BAMS-D-21-0125.1.

McDermid, S. S., R. Mahmood, M. J. Hayes, J. E. Bell, and Z. Lieberman, 2021: Minimizing trade-offs for sustainable irrigation. *Nat. Geosci.*, **14**, 706–709, https://doi.org/10.1038/s41561-021-00830-0.

——, and Coauthors, 2023: Irrigation in the Earth system. *Nat. Rev. Earth Environ.*, **4**, 435–453, https://doi.org/10.1038/s43017-023-00438-5.

Melillo, J. M., T. Richmond, and G. W. Yohe, 2014: *Climate Change Impacts in the United States: The Third National Climate Assessment*. U.S. Global Change Research Program, 841 pp.

Mueller, N. D., E. E. Butler, K. A. McKinnon, A. Rhines, M. Tingley, N. M. Holbrook, and P. Huybers, 2016: Cooling of US Midwest summer temperature extremes from cropland intensification. *Nat. Climate Change*, **6**, 317–322, https://doi.org/10.1038/nclimate2825.

——, A. Rhines, E. E. Butler, D. K. Ray, S. Siebert, N. M. Holbrook, and P. Huybers, 2017: Global relationships between cropland intensification and summer temperature extremes over the last 50 years. *J. Climate*, **30**, 7505–7528, https://doi.org/10.1175/JCLI-D-17-0096.1.

Nair, U. S., Y. Wu, J. Kala, T. J. Lyons, R. A. Pielke Sr., and J. M. Hacker, 2011: The role of land use change on the development and evolution of the west coast trough, convective clouds, and precipitation in southwest Australia. *J. Geophys. Res.*, **116**, D07103, https://doi.org/10.1029/2010JD014950.

——, and Coauthors, 2019: Influence of land cover and soil moisture based brown ocean effect on an extreme rainfall event from a Louisiana Gulf Coast tropical system. *Sci. Rep.*, **9**, 17136, https://doi.org/10.1038/s41598-019-53031-6.

NASA, 2021: Worldview. Accessed 15 November 2021, https://worldview.earthdata.nasa.gov/.

Na-Yemeh, D., R. Mahmood, G. Goodrich, K. Younger, K. Cary, and J. Durkee, 2020: Growing season air mass equivalent temperature (*TE*) in the east central USA. *Climate*, **8**, 95, https://doi.org/10.3390/cli8090095.

NCAR Earth Observing Laboratory, 1990: Integrated Surface Flux System (ISFS). UCAR, https://doi.org/10.5065/D6ZC80XJ.

——, 1997: Integrated Sounding System (ISS). UCAR, https://doi.org/10.5065/D6348HF9.

NOAA, 2020: June 2018 National Climate Report. NOAA, accessed 10 November 2020, https://www.ncdc.noaa.gov/sotc/national/201806.

Paul, S., S. Ghosh, R. Oglesby, A. Pathak, A. Chandrasekharan, and R. Ramsankaran, 2016: Weakening of Indian summer monsoon rainfall due to changes in land use land cover. *Sci. Rep.*, **6**, 32177, https://doi.org/10.1038/srep32177.

Pielke, R. A., Sr., C. Davey, and J. Morgan, 2004: Assessing "global warming" with surface heat content. *Eos, Trans. Amer. Geophys. Union*, **85**, 210–211, https://doi.org/10.1029/2004EO210004.

——, J. O. Adegoke, T. N. Chase, C. H. Marshall, T. Matsui, and D. Niyogi, 2007: A new paradigm for assessing the role of agriculture in the climate system and in climate change. *Agric. For. Meteor.*, **142**, 234–254, https://doi.org/10.1016/j.agrformet.2006.06.012.

——, and Coauthors, 2011: Land use/land cover changes and climate: Modeling analysis and observational evidence. *Wiley Interdiscip. Rev.: Climate Change*, **2**, 828–850, https://doi.org/10.1002/wcc.144.

——, R. Mahmood, and C. McAlpine, 2016: Land's complex role in climate change. *Phys. Today*, **69**, 40–46, https://doi.org/10.1063/PT.3.3364.

Qian, Y., M. Huang, B. Yang, and L. K. Berg, 2013: A modeling study of irrigation effects on surface fluxes and land–air–cloud interactions in the southern Great Plains. *J. Hydrometeor.*, **14**, 700–721, https://doi.org/10.1175/JHM-D-12-0134.1.

——, and Coauthors, 2020: Neglecting irrigation contributes to the simulated summertime warm-and-dry bias in the central United States. *npj Climate Atmos. Sci.*, **3**, 31, https://doi.org/10.1038/s41612-020-00135-w.

Rappin, E., and Coauthors, 2021: The Great Plains Irrigation Experiment (GRAINEX). *Bull. Amer. Meteor. Soc.*, **102**, E1756–E1785, https://doi.org/10.1175/BAMS-D-20-0041.1.

Rappin, E. D., R. Mahmood, U. S. Nair, and R. A. Pielke Sr., 2022: Land–atmosphere interactions during GRAINEX: Planetary boundary layer evolution in the presence of irrigation. *J. Hydrometeor.*, **23**, 1401–1417, https://doi.org/10.1175/JHM-D-21-0160.1.

Seidel, D. J., C. O. Ao, and K. Li, 2010: Estimating climatological planetary boundary layer heights from radiosonde observations: Comparison of methods and uncertainty analysis. *J. Geophys. Res.*, **115**, D16113, https://doi.org/10.1029/2009JD013680.

Seneviratne, S. I., D. Lüthi, M. Litschi, and C. Schär, 2006: Land–atmosphere coupling and climate change in Europe. *Nature*, **443**, 205–209, https://doi.org/10.1038/nature05095.

Sen Roy, S., R. Mahmood, D. Niyogi, M. Lei, S. A. Foster, K. G. Hubbard, E. Douglas, and R. A. Pielke Sr., 2007: Impacts of the agricultural green revolution-induced land use changes on air temperatures in India. *J. Geophys. Res.*, **112**, D21108, https://doi.org/10.1029/2007JD008834.

Sorooshian, S., A. AghaKouchak, and J. Li, 2014: Influence of irrigation on land hydrological processes over California. *J. Geophys. Res. Atmos.*, **119**, 13 137–13 152, https://doi.org/10.1002/2014JD022232.

Szilagyi, J., and T. E. Franz, 2020: Anthropogenic hydrometeorological changes at a regional scale: Observed irrigation–precipitation feedback (1979–2015) in Nebraska, USA. *Sustainable Water Resour. Manage.*, **6**, 1, https://doi.org/10.1007/s40899-020-00368-w.

Whitesel, D., R. Mahmood, P. Flanagan, E. Rappin, U. Nair, R. A. Pielke Sr., and M. Hayes, 2024: Impacts of irrigation on a precipitation event during GRAINEX in the High Plains Aquifer region. *Agric. For. Meteor.*, **345**, 109854, https://doi.org/10.1016/j.agrformet.2023.109854.

Winchester, J., R. Mahmood, W. Rodgers, F. Hossain, E. Rappin, J. Durkee, and T. Chronis, 2017: A model-based assessment of potential impacts of man-made reservoirs on precipitation. *Earth Interact.*, **21**, https://doi.org/10.1175/EI-D-16-0016.1.

Wurman, J., and Coauthors, 2021: The Flexible Array of Radars and Mesonets (FARM). *Bull. Amer. Meteor. Soc.*, **102**, E1499–E1525, https://doi.org/10.1175/BAMS-D-20-0285.1.

Yamada, T. J., and Y. Pokhrel, 2019: Effect of human-induced land disturbance on subseasonal predictability of near-surface variables using an atmospheric general circulation model. *Atmosphere*, **10**, 725, https://doi.org/10.3390/atmos10110725.

Yang, Z., and Coauthors, 2019: Irrigation impact on water and energy cycle during dry years over the United States using convection-permitting WRF and a dynamical recycling model. *J. Geophys. Res. Atmos.*, **124**, 11 220–11 241, https://doi.org/10.1029/2019JD030524.

——, and Coauthors, 2020: Understanding irrigation impacts on low-level jets over the Great Plains. *Climate Dyn.*, **55**, 925–943, https://doi.org/10.1007/s00382-020-05301-7.

Younger, K., R. Mahmood, G. Goodrich, R. A. Pielke Sr., and J. Durkee, 2019: Mesoscale surface equivalent temperature (*TE*) for east central USA. *Theor. Appl. Climatol.*, **136**, 65–75, https://doi.org/10.1007/s00704-018-2468-7.

Zhang, T., R. Mahmood, X. Lin, and R. A. Pielke Sr., 2019: Irrigation impacts on minimum and maximum surface moist enthalpy in the central Great Plains of the USA. *Wea. Climate Extremes*, **23**, 100197, https://doi.org/10.1016/j.wace.2019.100197.